

This is a repository copy of *Neutron capture measurement at the n TOF facility of the 204Tl and 205Tl s-process branching points*.

White Rose Research Online URL for this paper:

<https://eprints.whiterose.ac.uk/id/eprint/173553/>

Version: Published Version

---

**Article:**

(2020) Neutron capture measurement at the n TOF facility of the 204Tl and 205Tl s-process branching points. Journal of Physics: Conference Series. 012005. ISSN: 1742-6596

<https://doi.org/10.1088/1742-6596/1668/1/012005>

---

**Reuse**

This article is distributed under the terms of the Creative Commons Attribution (CC BY) licence. This licence allows you to distribute, remix, tweak, and build upon the work, even commercially, as long as you credit the authors for the original work. More information and the full terms of the licence here:

<https://creativecommons.org/licenses/>

**Takedown**

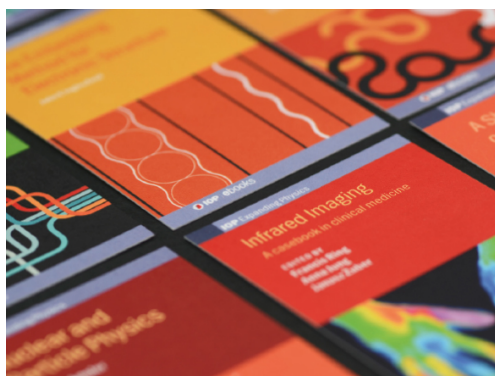
If you consider content in White Rose Research Online to be in breach of UK law, please notify us by emailing [eprints@whiterose.ac.uk](mailto:eprints@whiterose.ac.uk) including the URL of the record and the reason for the withdrawal request.

PAPER • OPEN ACCESS

## Neutron capture measurement at the n TOF facility of the $^{204}\text{Tl}$ and $^{205}\text{Tl}$ s-process branching points

To cite this article: A Casanovas *et al* 2020 *J. Phys.: Conf. Ser.* **1668** 012005

View the [article online](#) for updates and enhancements.



**IOP | ebooks™**

Bringing together innovative digital publishing with leading authors from the global scientific community.

Start exploring the collection—download the first chapter of every title for free.

## Neutron capture measurement at the n\_TOF facility of the $^{204}\text{Tl}$ and $^{205}\text{Tl}$ s-process branching points

A Casanovas<sup>1</sup>, A E Tarifeño-Saldivia<sup>1</sup>, C Domingo-Pardo<sup>2</sup>, F Calviño<sup>1</sup>, E Maugeri<sup>3</sup>, C Guerrero<sup>4</sup>, J Lerendegui-Marco<sup>4,2</sup>, R Dressler<sup>3</sup>, S Heinitz<sup>3</sup>, D Schumann<sup>3</sup>, J L Tain<sup>2</sup>, J M Quesada<sup>4</sup>, O Aberle<sup>5</sup>, V Alcayne<sup>6</sup>, S Amaducci<sup>7,8</sup>, J Andrzejewski<sup>9</sup>, L Audouin<sup>10</sup>, V Babiano-Suarez<sup>2</sup>, M Bacak<sup>5,11,12</sup>, J Balibrea<sup>2</sup>, M Barbagallo<sup>5,13</sup>, S Bennett<sup>14</sup>, E Berthoumieux<sup>12</sup>, D Bosnar<sup>15</sup>, A S Brown<sup>16</sup>, M Busso<sup>17,18</sup>, M Caamaño<sup>19</sup>, L Caballero<sup>2</sup>, M Calviani<sup>5</sup>, D Cano-Ott<sup>6</sup>, F Cerutti<sup>5</sup>, E Chiaveri<sup>5,14</sup>, N Colonna<sup>13</sup>, G P Cortés<sup>1</sup>, M A Cortés-Giraldo<sup>4</sup>, L Cosentino<sup>7</sup>, S Cristallo<sup>17,20</sup>, L A Damone<sup>13,21</sup>, P J Davies<sup>14</sup>, M Diakaki<sup>22</sup>, M Dietz<sup>23</sup>, Q Ducasse<sup>24</sup>, E Dupont<sup>12</sup>, I Durán<sup>19</sup>, Z Eleme<sup>25</sup>, B Fernández-Domínguez<sup>19</sup>, A Ferrari<sup>5</sup>, I Ferro-Gonçalves<sup>26</sup>, P Finocchiaro<sup>7</sup>, V Furman<sup>27</sup>, R Garg<sup>23</sup>, A Gawlik<sup>9</sup>, S Gilardoni<sup>5</sup>, K Göbel<sup>28</sup>, E González-Romero<sup>6</sup>, F Gunsing<sup>12</sup>, J Heyse<sup>29</sup>, D G Jenkins<sup>16</sup>, E Jericha<sup>11</sup>, U Jiri<sup>3</sup>, A Junghans<sup>30</sup>, Y Kadi<sup>5</sup>, F Käppeler<sup>31</sup>, A Kimura<sup>32</sup>, I Knapová<sup>33</sup>, M Kokkoris<sup>22</sup>, Y Kopatch<sup>27</sup>, M Krtićka<sup>33</sup>, D Kurtulgil<sup>28</sup>, I Ladarescu<sup>2</sup>, C Lederer-Woods<sup>23</sup>, S.-J Lonsdale<sup>23</sup>, D Macina<sup>5</sup>, A Manna<sup>34,35</sup>, T Martínez<sup>6</sup>, A Masi<sup>5</sup>, C Massimi<sup>34,35</sup>, P F Mastinu<sup>36</sup>, M Mastromarco<sup>5</sup>, A Mazzone<sup>13,37</sup>, E Mendoza<sup>6</sup>, A Mengoni<sup>38,34</sup>, V Michalopoulou<sup>5,22</sup>, P M Milazzo<sup>39</sup>, M A Millán-Callado<sup>4</sup>, F Mingrone<sup>5</sup>, J Moreno-Soto<sup>12</sup>, A Musumarra<sup>7,8</sup>, A Negret<sup>40</sup>, F Ogállar<sup>41</sup>, A Oprea<sup>40</sup>, N Patronis<sup>25</sup>, A Pavlik<sup>42</sup>, J Perkowski<sup>9</sup>, C Petrone<sup>40</sup>, L Piersanti<sup>17,20</sup>, E Pirovano<sup>24</sup>, I Porras<sup>41</sup>, J Praena<sup>41</sup>, D Ramos Doval<sup>10</sup>, R Reifarth<sup>28</sup>, D Rochman<sup>3</sup>, C Rubbia<sup>5</sup>, M Sabaté-Gilarte<sup>4,5</sup>, A Saxena<sup>43</sup>, P Schillebeeckx<sup>29</sup>, A Sekhar<sup>14</sup>, A G Smith<sup>14</sup>, N Sosnin<sup>14</sup>, P Sprung<sup>3</sup>, A Stamatopoulos<sup>22</sup>, G Tagliente<sup>13</sup>, L Tassan-Got<sup>5,22,10</sup>, B Thomas<sup>28</sup>, P Torres-Sánchez<sup>41</sup>, A Tsinganis<sup>5</sup>, S Urlass<sup>5,30</sup>, S Valenta<sup>33</sup>, G Vannini<sup>34,35</sup>, V Variale<sup>13</sup>, P Vaz<sup>26</sup>, A Ventura<sup>34</sup>, D Vescovi<sup>17,44</sup>, V Vlachoudis<sup>5</sup>, R Vlastou<sup>22</sup>, A Wallner<sup>45</sup>, P J Woods<sup>23</sup>, T J Wright<sup>14</sup>, P Žugec<sup>15</sup> and U Koester<sup>46</sup>

<sup>1</sup> Universitat Politècnica de Catalunya, Spain

<sup>2</sup> Instituto de Física Corpuscular, CSIC - Universidad de Valencia, Spain

<sup>3</sup> Paul Scherrer Institut (PSI), Villigen, Switzerland



*Neutron capture measurement in  $^{204}\text{Tl}$  and  $^{205}\text{Tl}$  at n-TOF (CERN)*<sup>4</sup> Universidad de Sevilla, Spain<sup>5</sup> European Organization for Nuclear Research (CERN), Switzerland<sup>6</sup> Centro de Investigaciones Energéticas Medioambientales y Tecnológicas (CIEMAT), Spain<sup>7</sup> INFN Laboratori Nazionali del Sud, Catania, Italy<sup>8</sup> Dipartimento di Fisica e Astronomia, Università di Catania, Italy<sup>9</sup> University of Lodz, Poland<sup>10</sup> IPN, CNRS-IN2P3, Univ. Paris-Sud, Université Paris-Saclay, F-91406 Orsay Cedex, France<sup>11</sup> Technische Universität Wien, Austria<sup>12</sup> CEA Saclay, Irfu, Université Paris-Saclay, Gif-sur-Yvette, France<sup>13</sup> Istituto Nazionale di Fisica Nucleare, Bari, Italy<sup>14</sup> University of Manchester, United Kingdom<sup>15</sup> Department of Physics, Faculty of Science, University of Zagreb, Croatia<sup>16</sup> University of York, United Kingdom<sup>17</sup> Istituto Nazionale di Fisica Nucleare, Perugia, Italy<sup>18</sup> Dipartimento di Fisica e Geologia, Università di Perugia, Italy<sup>19</sup> University of Santiago de Compostela, Spain<sup>20</sup> Istituto Nazionale di Astrofisica - Osservatorio Astronomico d'Abruzzo, Italy<sup>21</sup> Dipartimento di Fisica, Università degli Studi di Bari, Italy<sup>22</sup> National Technical University of Athens, Greece<sup>23</sup> School of Physics and Astronomy, University of Edinburgh, United Kingdom<sup>24</sup> Physikalisch-Technische Bundesanstalt (PTB), Bundesallee 100, 38116 Braunschweig, Germany<sup>25</sup> University of Ioannina, Greece<sup>26</sup> Instituto Superior Técnico, Lisbon, Portugal<sup>27</sup> Joint Institute for Nuclear Research (JINR), Dubna, Russia<sup>28</sup> Goethe University Frankfurt, Germany<sup>29</sup> European Commission, Joint Research Centre, Geel, Retieseweg 111, B-2440 Geel, Belgium<sup>30</sup> Helmholtz-Zentrum Dresden-Rossendorf, Germany<sup>31</sup> Karlsruhe Institute of Technology, Campus North, IKP, 76021 Karlsruhe, Germany<sup>32</sup> Japan Atomic Energy Agency (JAEA), Tokai-mura, Japan<sup>33</sup> Charles University, Prague, Czech Republic<sup>34</sup> Istituto Nazionale di Fisica Nucleare, Sezione di Bologna, Italy<sup>35</sup> Dipartimento di Fisica e Astronomia, Università di Bologna, Italy<sup>36</sup> Istituto Nazionale di Fisica Nucleare, Sezione di Legnaro, Italy<sup>37</sup> Consiglio Nazionale delle Ricerche, Bari, Italy<sup>38</sup> Agenzia nazionale per le nuove tecnologie, l'energia e lo sviluppo economico sostenibile (ENEA), Bologna, Italy<sup>39</sup> Istituto Nazionale di Fisica Nucleare, Trieste, Italy<sup>40</sup> Horia Hulubei National Institute of Physics and Nuclear Engineering (IFIN-HH), Bucharest<sup>41</sup> University of Granada, Spain<sup>42</sup> University of Vienna, Faculty of Physics, Vienna, Austria<sup>43</sup> Bhabha Atomic Research Centre (BARC), India<sup>44</sup> Gran Sasso Science Institute (GSSI), L'Aquila, Italy<sup>45</sup> Australian National University, Canberra, Australia<sup>46</sup> Institute Laue Langevin (ILL), Grenoble, FranceE-mail: [adria.casanovas@upc.edu](mailto:adria.casanovas@upc.edu)

*Neutron capture measurement in  $^{204}\text{Tl}$  and  $^{205}\text{Tl}$  at n\_TOF (CERN)*

October 2019

**Abstract.** Neutron capture cross sections are one of the fundamental nuclear data in the study of the s (*slow*) process of nucleosynthesis. More interestingly, the competition between the capture and the decay rates in some unstable nuclei determines the local isotopic abundance pattern. Since decay rates are often sensible to temperature and electron density, the study of the nuclear properties of these nuclei can provide valuable constraints to the physical magnitudes of the nucleosynthesis stellar environment. Here we report on the capture cross section measurement of two thallium isotopes,  $^{204}\text{Tl}$  and  $^{205}\text{Tl}$  performed by the time-of-flight technique at the n\_TOF facility at CERN. At some particular stellar s-process environments, the decay of both nuclei is strongly enhanced, and determines decisively the abundance of two s-only isotopes of lead,  $^{204}\text{Pb}$  and  $^{205}\text{Pb}$ . The latter, as a long-lived radioactive nucleus, has potential use as a chronometer of the last s-process events that contributed to final solar isotopic abundances.

**1. Introduction**

Approximately half of the solar elemental abundances heavier than iron are produced by the so-called s-process of stellar nucleosynthesis. This is characterized by successive neutron capture and beta decay reactions, following the path of the valley of stability. An up to date review of the s-process, including a detailed analysis of the stellar scenarios where it occurs, can be found in [1]. Elements with  $A > 90$  are mainly produced in the *main* s-process, which takes places in the Asymptotic Giant Branch (AGB) phase of low mass ( $1.5 - 3 M_{\odot}$ ), thermally pulsating stars. During the AGB phase, s-process happens in two main environments, characterized by different physical conditions. Between two Thermal Pulse (TP) episodes, H is burned radiatively in a shell at the bottom of the convective envelope. In the ashes of the H-burning shell, conditions are such that a  $^{13}\text{C}$  pocket forms, and neutrons are released by the  $^{13}\text{C}(\alpha, n)$  reaction. When temperature approaches  $\sim 0.9 \cdot 10^8$  K (corresponding to  $kT \sim 8$  keV), neutron densities of  $\sim 10^7 \text{ cm}^{-3}$  trigger the s-process. But in the recurrent TP episodes, the convective flash fusion of the accumulated He-shell during the interpulse rises the temperature up to  $\sim 3 \cdot 10^8$  K (corresponding to  $kT \sim 26$  keV). This enables the release of neutrons by the partial activation of the  $^{22}\text{Ne}(\alpha, n)$  reaction. Although these events last for a few years, neutron densities can reach up to  $\sim 10^{10} \text{ cm}^{-3}$ , changing the isotopic patterns around some particular isotopes.

Along the s-process path, some nuclei are radioactive, with half-lives from a few years to thousands of years. In these, the neutron capture rates may compete with their decay rates. In some cases, the high temperature reached during the TP can enhance the decay of this nuclei, changing considerably their capture-to-decay ratio. When this occurs, the usual path of the nucleosynthesis process is changed, which affects the abundances of stable nuclei immediately following the unstable species. Hence, by affecting local isotopic ratios, these nuclei -which receive the name of *branching points*-

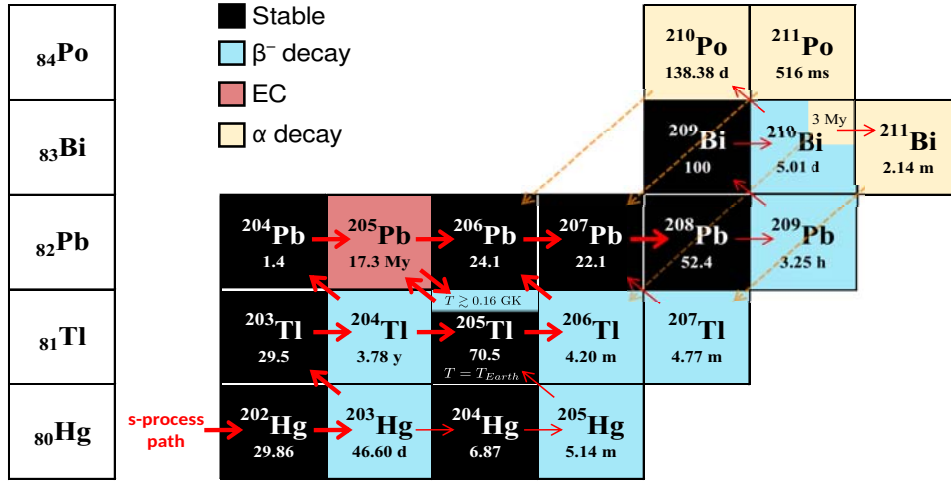
*Neutron capture measurement in  $^{204}\text{Tl}$  and  $^{205}\text{Tl}$  at n-TOF (CERN)*

Figure 1: The s-process in its termination area, in the mass region  $A = 203 - 210$ . Thick red arrows represent the main s-process path, while thin arrows indicate secondary paths. From  $\sim 1.6 \cdot 10^8$  K, a temperature which is easily reached and surpassed during TP events, the  $^{205}\text{Tl}$  decay becomes relevant, and even exceeds that of  $^{205}\text{Pb}$ .

become probes of the stellar conditions where they are produced. However, to achieve that it is necessary to know their neutron capture cross section, and  $\beta^-$  decay rates.

$^{204}\text{Tl}$  and  $^{205}\text{Tl}$  are relevant branching points because of their situation in the endpoint of the s-process path (figure 1). This region, which comprises nuclei with  $A = 203 - 210$ , is of special interest. Due to the proximity of the neutron shell closure,  $^{205}\text{Tl}$ ,  $^{206}\text{Pb}$ ,  $^{207}\text{Pb}$ , and especially the double magic nucleus  $^{208}\text{Pb}$ , form the third s-process peak of abundances. In addition,  $^{204}\text{Pb}$  and the radioactive  $^{205}\text{Pb}$  are produced only by the s-process. The latter, with a half-life of 17.3 My, has several cosmochemical applications [2]. On top of that, it has the potential to be used as a chronometer of the last s-process events that contributed to the Solar System [3][4]. The TP physical conditions enhance strongly the decay of  $^{204}\text{Tl}$  to  $^{204}\text{Pb}$ , and activate that of the terrestrially stable  $^{205}\text{Tl}$  to  $^{205}\text{Pb}$ , by bound state  $\beta^-$  decay [3]. Therefore, the capture cross section of both, by competing with their decay rate, is crucial to determine the final abundances of  $^{204}\text{Pb}$  and  $^{205}\text{Pb}$ .

In this work we present the neutron capture experiments on  $^{204}\text{Tl}$  and  $^{205}\text{Tl}$  performed at the n-TOF facility at CERN, in the neutron energy range of astrophysical interest (1 eV to 100 keV). The experiments were carried out in 2015 and 2018, respectively.

*Neutron capture measurement in  $^{204}\text{Tl}$  and  $^{205}\text{Tl}$  at n-TOF (CERN)***2. Experiment***2.1. Samples*

The sample employed to measure the  $^{204}\text{Tl}(n,\gamma)$  reaction was a 260 mg pellet of  $\text{Tl}_2\text{O}_3$ , enriched up to 4% in  $^{204}\text{Tl}$  by neutron irradiation in the ILL (Grenoble) nuclear reactor. The total mass of  $^{204}\text{Tl}$  at the time of the experiment was 9 mg. It was encapsulated in a quartz ampoule to reduce the  $\beta$  radiation, which caused a secondary bremsstrahlung background. Total  $^{204}\text{Tl}$  activity at the time of the experiment was 150 GBq, in addition to 370 kBq of  $^{60}\text{Co}$ . The presence of the latter arose from activation of a small impurity ( $< 0.3$  ppm) of natural Co in the  $\text{Tl}_2\text{O}_3$  seed pellet. The two gamma rays, with energies 1.17 and 1.33 MeV, coming from the  $^{60}\text{Co}$  decay were the main contributor to photon background at energies above 800 keV. Another issue was that, after irradiation, there was high uncertainty in the exact sample position in the quartz container, and close manipulation was not possible. Therefore, in order to guarantee that most of the sample would be irradiated upon insertion in the neutron beam, a remote gamma-ray scanning of the ampoule was carried out. More details can be found in [5].

For the  $^{205}\text{Tl}(n,\gamma)$  measurement, a  $>99\%$  enriched  $\text{Tl}_2\text{O}_3$  sample had been prepared. However, in the first hours of measurement a high contamination of bromine was identified in the data. Bromine isotopes have very high number of capture resonances in the same range of  $^{205}\text{Tl}$ , and thus the measurement was not feasible under these conditions. Fortunately, thanks to the radiochemistry laboratory of PSI an alternative sample of natural thallium could be produced in time for the experiment. Natural thallium contains 70.5% of  $^{205}\text{Tl}$  whereas the remaining 29.5% is  $^{203}\text{Tl}$ . The latter has a high capture cross section as well, but it had been measured recently for the  $^{204}\text{Tl}$  campaign. Furthermore, capture resonance spacing is relatively high in thallium isotopes, and thus the chance of overlapping resonances is low. The final sample had a mass of 3.6 g of  $^{\text{nat}}\text{Tl}$ , which corresponds to 2.6 g of  $^{205}\text{Tl}$ . It was pressed into a cylindrical pellet of radius 1 cm, and thickness of 2 mm. Due to the high toxicity of thallium, it was enclosed in a PEEK capsule for the experiment.

*2.2. Measurement and analysis methods*

The capture experiments were conducted at the n-TOF Experimental Area 1 (EAR1). At n-TOF neutrons are produced by impinging pulses of  $7 \cdot 10^{12}$  protons, accelerated to 20 GeV/c by the Proton Synchrotron (PS), in a lead target. In the ensuing spallation reactions, about 300 neutrons per proton are released, which makes n-TOF the most luminous facility of its kind. The energy of the neutrons is determined by the time-of-flight technique at the experimental area. Thanks to the long flight path of 184 m, a very high resolution in neutron energy is attained in a wide energy range. The prompt gamma rays that follow the neutron capture are counted by means of four  $\text{C}_6\text{D}_6$  detectors, which have been optimized specifically for a very low neutron sensitivity. The raw counting rate is converted into reaction yield by applying the Pulse Height

*Neutron capture measurement in  $^{204}\text{Tl}$  and  $^{205}\text{Tl}$  at n-TOF (CERN)*

Weighting Technique [6][7], and the absolute yield normalization is obtained by applying the gold saturated resonance method [8]. Background signals are subtracted from the yield, but this requires identifying the different sources. First of all, for  $^{204}\text{Tl}$  the huge photon background coming from the sample activity is measured by recording data without beam. There are two other sources of background photons, which are estimated separately: those coming in the beam and scattered by the sample, and those produced by the capture, anywhere in the experimental hall, arising from neutrons previously scattered in the sample. In the first case, the background is estimated by employing a natural lead sample, which is a high photon scatterer. In the second case, a light element like  $^{12}\text{C}$  which scatters mostly neutrons, is employed. Finally, the contribution of the different sample containers was measured using dummy samples. The n-TOF neutron flux is known with a 2% precision from 100 eV to 10 keV, and with a 5% in the 10 to 100 keV range [9]. The neutron counting rate is continuously monitored along the measurement by four silicon detectors.

The capture yield, in the Resolved Resonance Region (RRR), has been analysed with the bayesian R-Matrix analysis tool SAMMY [10]. In the RRR, SAMMY reconstructs the theoretical cross section using the Reich-Moore approximation to the R-Matrix formalism. It includes corrections for thermal broadening and sample thickness effects, like multiple-scattering and self-shielding.

### 3. Preliminary results and outlook

We report here on the first time ever direct measurement of  $^{204}\text{Tl}$  capture resonances up to 1 keV. R-Matrix fits of the resonances, compared to those predicted by the evaluations, are plotted in figures 2 and 3. Final determination of the resonance areas, limited up to a few keV, is being currently carried out. The main challenge for the analysis is the very low total mass of  $^{204}\text{Tl}$  present, together with the dominant presence of  $^{203}\text{Tl}$  resonances (figure 3). We expect that the new data will be useful to set an upper limit to evaluated cross section libraries, and will aid future calculations of the cross section for astrophysical applications.

Concerning the  $^{205}\text{Tl}(n,\gamma)$  measurement, a preliminary analysis of the yield shows that clear identification of capture resonances is possible up to at least 100 keV (figure 4). Additionally, we expect to provide an averaged cross section for the Unresolved Resonance Region beyond 100 keV. All this combined together, should allow for a reliable determination of the Maxwellian Averaged Cross Section (MACS) at 25-30 keV, the range of  $kT$  temperatures reached during the TP stellar events, when the decay of  $^{205}\text{Tl}$  to  $^{205}\text{Pb}$  is more strongly enhanced. It is opportune noting here that a measurement of the bound state  $\beta^-$  decay of highly ionized  $^{205}\text{Tl}$  is scheduled for next year at the Experimental Storage Ring (ESR) at GSI (Germany) [11]. The knowledge of both the decay rate and the capture cross section should allow for a comprehensive analysis of the role of the  $^{205}\text{Tl}$  during s-process nucleosynthesis.



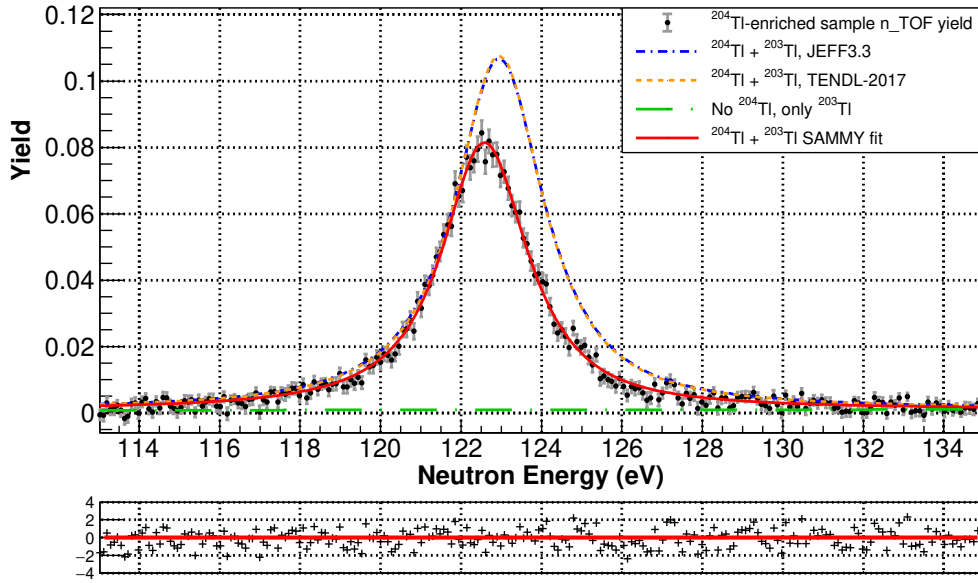
*Neutron capture measurement in  $^{204}\text{Tl}$  and  $^{205}\text{Tl}$  at n-TOF (CERN)*

Figure 2: Fit with SAMMY of the 122 eV resonance of  $^{204}\text{Tl}(n,\gamma)$  in the  $^{204}\text{Tl}$ -enriched sample data (red solid line). For comparison, the evaluated cross section for the JEFF-3.3 (based on TENDL-2015) and TENDL-2017 evaluations is also plotted.

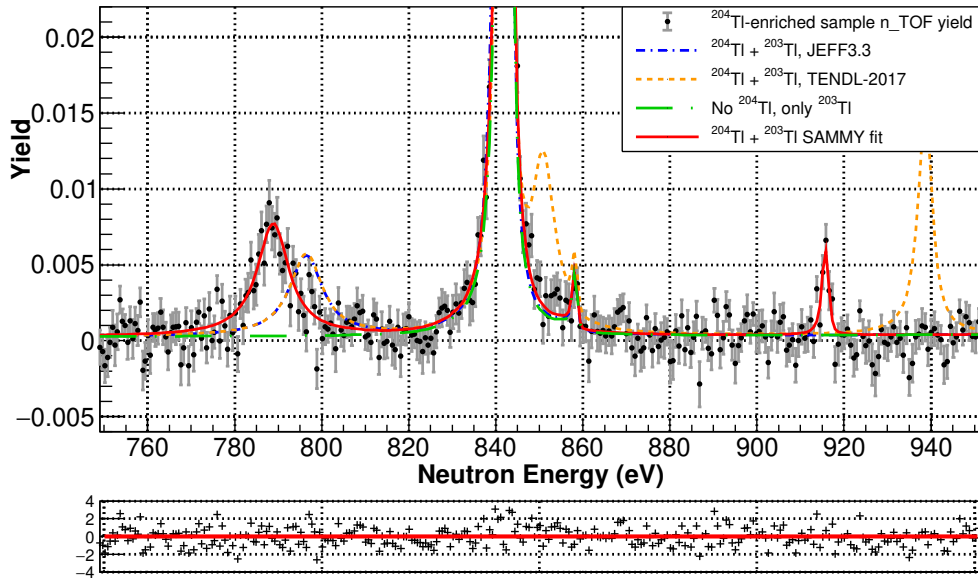


Figure 3: Fit of the  $^{204}\text{Tl}(n,\gamma)$  resonances at 789 and 915 eV. The green dashed line corresponds to a fit without  $^{204}\text{Tl}$  resonances of the  $^{204}\text{Tl}$ -enriched sample data. The resonances at 842 and 857 eV belong to capture in  $^{203}\text{Tl}$ .

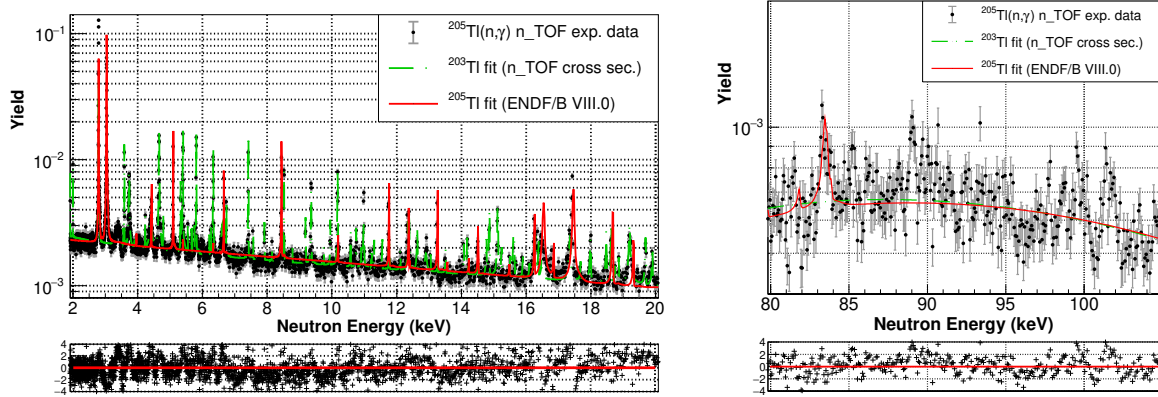
*Neutron capture measurement in  $^{204}\text{Tl}$  and  $^{205}\text{Tl}$  at n-TOF (CERN)*

Figure 4: (a): Yield of the  $^{205}\text{Tl}(n,\gamma)$  reaction in the range from 2 to 20 keV. A Very preliminary fit of  $^{205}\text{Tl}$  capture resonances is plotted (solid red line), using the ENDF/B-VIII.0 evaluation. The green dashed line are  $^{203}\text{Tl}$  capture resonances, employing the data from the 2015  $^{203}\text{Tl}(n,\gamma)$  n-TOF measurement. (b) The experimental  $^{205}\text{Tl}(n,\gamma)$  yield close to 100 keV, where resonances are clearly visible at 89, 99 and 102 keV.

*Neutron capture measurement in  $^{204}\text{Tl}$  and  $^{205}\text{Tl}$  at n-TOF (CERN)***References**

- [1] Käppeler F, Gallino R, Bisterzo S & Aoki W 2011 *Rev. Mod. Phys.* **83**(1) 157–193 URL <https://link.aps.org/doi/10.1103/RevModPhys.83.157>
- [2] Palk C *et al.* 2018 *Meteorit. Planet. Sci.* **53** 167–186 (Preprint <https://onlinelibrary.wiley.com/doi/pdf/10.1111/maps.12989>)
- [3] Yokoi K, Takahashi K & Arnould M 1985 *Astron. Astrophys.* **145** 339–346
- [4] Baker R, Schnebler M, Rehkemper M, Williams H & Halliday A 2010 *Earth Planet. Sci. Lett.* **291** 39 – 47 ISSN 0012-821X URL <http://www.sciencedirect.com/science/article/pii/S0012821X10000075>
- [5] Tarifeño-Saldivia A 2015 Characterization of the spatial distribution of high radioactive targets for capture cross section measurements of s-process branching nuclei at CERN n-TOF *CHANDA Workshop on Target Preparation*
- [6] Macklin R L & Gibbons J H 1967 *Phys. Rev.* **159**(4) 1007–1012 URL <https://link.aps.org/doi/10.1103/PhysRev.159.1007>
- [7] Abbondanno U *et al.* 2004 *Nucl. Instrum. Methods Phys. Res., Sect. A* **521** 454 – 467 ISSN 0168-9002 URL <http://www.sciencedirect.com/science/article/pii/S0168900203029425>
- [8] Macklin R L, Halperin J & Winters R R 1979 *Nucl. Instrum. Methods* **164** 213 – 214 ISSN 0029-554X URL <http://www.sciencedirect.com/science/article/pii/0029554X79904579>
- [9] Barbagallo M *et al.* 2013 *Eur. Phys. J. A* **49** 156 ISSN 1434-601X URL <https://doi.org/10.1140/epja/i2013-13156-x>
- [10] Larson N M 2008 Updated user’s guide for sammy: Multilevel r-matrix fits to neutron data using bayes’ equations Tech. rep. Oak Ridge National Laboratory
- [11] Litvinov Y A 2017 Proposal E121: ”measurement of the bound-state beta decay of bare  $^{205}\text{Tl}$  ions” Tech. rep. GSI